J. KOSAE Vol. 19, No. E 3 (2003) pp. 137~148
Journal of Korean Society for Atmospheric Environment

# Assessment of the Nitrate Radical Chemistry and Chemical Composition on Jeju Island during the Asian Pollution Period in the Spring of 2001

Zang-Ho Shon*, Ki-Hyun Kim[1)], Keith N. Bower[2)],
Gangwoong Lee[3)] and Jiyoung Kim[4)]

*Dept. of Environmental Engineering, Dong-Eui University, Korea,*
[1)]*Dept. of Earth & Environmental Sciences, Sejong University, Korea,*
[2)]*Physics Dept., UMIST, United Kingdom,*
[3)]*Dept. of Environmental Sciences, Hankook University of Foreign Studies, Korea,*
[4)]*Meterological Research Institute, Korea*

(Received 31 July 2003, accepted 21 October 2003)

## Abstract

In this study, we examined the influence of long-range transport of dust particles and air pollutants on the photochemistry of $NO_3$ on Jeju Island, Korea (33.17° N, 126.10° E) during the Asian Dust-Storm (ADS) period of April 2001. Three ADS events were observed during the periods of 10~12, 13~14, and 25~26 April. Average concentration level of nighttime $NO_3$ on Jeju Island during the ADS period was estimated to be about $2 \times 10^8$ molecules $cm^{-3}$ (~9 pptv). Decreases in $NO_3$ levels during the ADS period was likely to be determined mainly by the enhancement of the $N_2O_5$ heterogeneous reaction on dust aerosol surfaces. The reaction of $N_2O_5$ on aerosol surfaces was a more important sink for nighttime $NO_3$ during the ADS due to the significant loading of dust particles. The reaction of $NO_3$ with NMHCs and the gas-phase reaction of $N_2O_5$ with water vapor were both significant loss mechanisms during the study period, especially during the NADS. However, dry deposition of these oxidized nitrogen species and a heterogeneous reaction of $NO_3$ were of no importance. Short-term observations of $O_3$, $NO_2$, DMS, and $SO_2$ in the MBL indicated that concentrations of most of these chemical species were different between the ADS and non-Asian-Dust-Storm (NADS) periods, implying that their levels were affected sensitively by the differences in air mass trajectories.

**Key words** : $NO_3$, Asian dust storm, ACE-Asia, Jeju Island

## 1. INTRODUCTION

Both hydroxyl (OH) and hydroperoxyl ($HO_2$) radicals can play a significant role in the chemistry of the daytime troposphere (Wayne, 1991). By contrast, nitrate radical ($NO_3$) plays an important role in the chemistry of the nighttime troposphere, serving as an oxidizing agent for various hydrocarbons and as a medium for the removal of $NO_x$ ($NO+NO_2$) in the form of nitric acid (Wayne, 1991). The nitrate radical is produced by the reaction of $NO_2$ with $O_3$:

* Corresponding author.
Tel : +82-(0)51-890-2078, E-mail : zangho@dongeui.ac.kr

$$NO_2+O_3 \rightarrow NO_3+O_2 \quad (1)$$

For instance, the nitrate is a dominant oxidizing agent of dimethyl sulfide (DMS) in the marine boundary layer (MBL) during the nighttime (Wayne *et al.*, 1991).

It is speculated that the atmospheric photochemistry of chemical species in remote MBL can be affected by long-range transport of dust particles accompanied by significantly high loadings of anthropogenic pollutants. In East Asia, dust storms tend to originate in desert areas of northwestern China during the spring; their impacts have been observed not only in nearby Asian countries (e.g., Korea and Japan) but also as far away as the Aleutians and North America (Jaffee *et al.*, 1999). $SO_2$ and NO levels on Jeju Island (formerly known as Cheju Island) were found to be as high as a few ppbv in the atmospheric boundary layer (ABL) during the Asian dust-storm (ADS) period due to the continental outflow of air pollutants from China (Kim *et al.*, 1998). Photochemical oxidation of atmospheric species can be facilitated during the ADS period because of the enhancement of nitrogen oxide levels. DMS oxidation by $NO_3$ can be significant during the ADS period, compared to the remote MBL where OH mainly regulates its oxidation. In the case of polluted air mass, nitrate radicals were mainly removed indirectly through reactions of $N_2O_5$, either in the gas phase or on aerosol surfaces. However, reactions of $NO_3$ with unsaturated hydrocarbons also contributed significantly to its loss (Geyer *et al.*, 2001b; Allan *et al.*, 1999; Carslaw *et al.*, 1997). In clean marine air masses, DMS was the dominant scavenger of $NO_3$ (Allan *et al.*, 2000; Carslaw *et al.*, 1997).

In this paper, we present the stepwise analysis of the photochemistry $NO_3$ using ground-based measurement data sets obtained on Jeju Island (see Fig. 1) during ACE-Asia. First, we summarize the observational data sets used in this study. Secondly, detailed descriptions of the model used for the calculations of $NO_3$ concentrations are presented. Thirdly, the issue of $NO_3$ budgets in the case of high $NO_x$ environments is explored in relation to the impact of the ADS on their photochemistry. Finally, we also attempt to account for the factors governing their photochemistry in the ABL and to determine the contribution of the ADS on $NO_3$ levels. To our knowledge, this study is the first attempt to elucidate the photochemistry of $NO_3$ on Jeju Island in relation to ADS events.

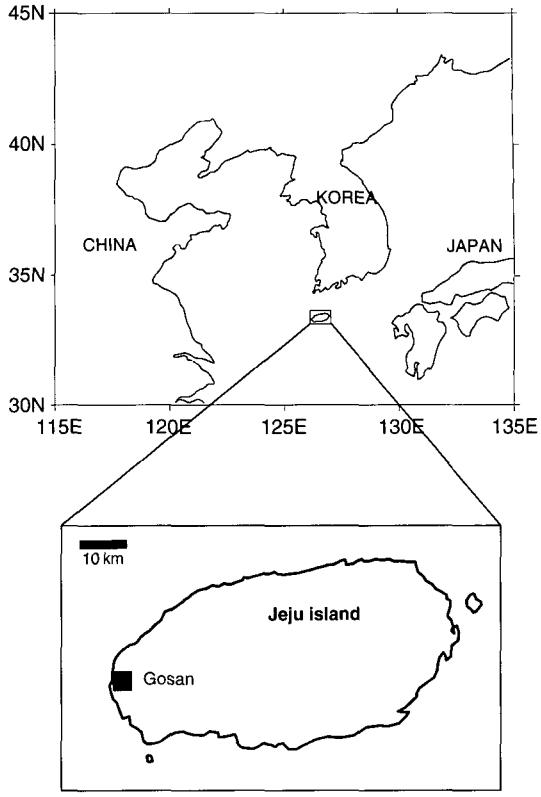


**Fig. 1. Location of a sampling site on Gosan, Jeju Island (33.17° N, 126.10° E).**

## 2. OBSERVATIONAL DATA

This study is based on the measurements of several atmospheric trace gases and relevant meteorological parameters made during an intensive ground-based field study for the Asian Pacific Regional Aerosol Characterization Experiment (ACE-Asia). As part of ACE-Asia, an intensive field campaign took place off the

**Table 1. A statistical summary of 6-hr averaged input variables.**

| Variables | ADS period | | | | NADS period | | | |
|---|---|---|---|---|---|---|---|---|
| | 00:00 | 06:00 | 12:00 | 18:00 | 00:00 | 06:00 | 12:00 | 18:00 |
| T(°C) | 11.4 | 11.2 | 13.0 | 12.6 | 13.0 | 12.4 | 16.2 | 15.7 |
| Dew Point(°C) | 6.8 | 6.1 | 5.2 | 6.3 | 8.6 | 7.9 | 9.3 | 9.3 |
| [CO] (ppbv) | 265 | 274 | 305 | 213 | 148 | 168 | 149 | 133 |
| [$NO_2$] (ppbv) | 3.8 | 3.4 | 4.7 | 4.6 | 4.3 | 4.3 | 4.5 | 4.4 |
| [$O_3$] (ppbv) | 47 | 46 | 46 | 50 | 44 | 42 | 47 | 50 |
| [DMS] (pptv) | 19 | 25 | 41 | 30 | 11 | 21 | 17 | 15 |
| [$SO_2$] (ppbv) | 0.85 | 0.83 | 1.31 | 0.79 | 0.36 | 0.46 | 0.53 | 0.49 |

coast of Gosan (formerly known as Kosan), Jeju (33.17 °N, 126.10° E) in the month of April 2001 (Kim *et al.*, 2003).

In this field program, we made measurements of trace gases such as $O_3$, CO, NO, $NO_2$, and $SO_2$ that were measured using unmodified commercial units. The instruments were particularly well suited to taking measurements in semi-polluted/continentally-influenced situations, but were close to their detection limit particularly in clean air masses. The analysis of DMS in the air was also made by an on-line GC system interfaced with a Pulsed Flame Photometric Detector (PFPD) modified from Swan and Ivey (1999). The detection limit for the system was found to be 20 pg of S that corresponds to about 2 pptv of mixing ratio (at total sampled volume of ~4 *l*). Detailed discussion on the DMS measurements is given in Kim *et al.* (2003). Each of our target species was measured every minute interval, except for DMS (every 15 min.). NO and $NO_2$ were measured using a Thermo Environmental Instruments Model 42C Chemiluminescence NO-$NO_2$-$NO_x$ analyzer with a detection limit (DL) of 0.4 ppbv at a precision of ±0.4 ppbv. $O_3$ was measured using a Monitor Labs Model 8810 Ozone analyzer with a DL of ±2 ppbv at a precision of ±2 ppbv. $SO_2$ was measured using a Thermo Environmental Instruments Model 43S pulsed fluorescence $SO_2$ analyzer with a DL of 0.1 ppbv at a response time of 4 minutes. CO was measured using a Thermo Environmental Instruments Model 48C with a DL of 0.04 ppmv at an average time of 10~300 s and at a precision of 0.1 ppmv. The Jeju Meteorological Station measured most of the basic meteorological parameters during April 2001.

Ten-minute averaged concentrations for the photochemical species were used as input variables for the photochemical box model (PCBM). Table 1 shows 6-hour averaged values of all input variables during both the ADS and Non-Asian-Dust-Storm (NADS) periods. Note that most of the NO concentrations were at or below the DL. Therefore, model runs were carried out using the model calculated NO values. The calculation of NO values was based on the photostationary state ratio of $NO_2$/NO by considering the partitioning of $NO_x$ according to Eq. (2):

$$\frac{[NO_2]}{[NO]} = \frac{(k_{O_3}[O_3]+k_{HO_2}[HO_2]+k_{CH_3O_2}[CH_3O_2]+k_{RO_2}[RO_2])}{J_{NO_2}} \quad (2)$$

where [X] (X = NO, $NO_2$, $O_3$, $HO_2$, $CH_3O_2$, and $RO_2$) corresponds to the concentration of the chemical species X; k denotes a reaction rate coefficient of a corresponding reaction; and $J_{NO_2}$ denotes the photolysis rate coefficient of $NO_2$. The photostationary state is a steady state reached by a reacting chemical system when sunlight has been absorbed by at least one of the components. At this state the rates of formation and destruction are equal for each of the transient molecular entities formed. Detailed discussion on the J values is given in section 3.

## 3. MODEL DESCRIPTION

The PCBM was employed to generate diurnal profile $NO_3$. For the PCBM, a pseudo-steady-state approxi-

mation (PSSA) was used to calculate concentrations of relatively short-lived species (OH, NO, $HO_2$, $CH_3O_2$, etc.). This approach is expected to lead to a reasonable representation of the short-lived species. The PSSA is based on the presumption that the formation and destruction rates of the chemical species are equal:

$$\frac{d[X]}{dt} = P(X) - L(X)[X] \approx 0 \quad (3)$$

$$[X]_{PSSA} \approx \frac{P(X)}{L(X)} \quad (4)$$

where P(X) is the sum of the production rates of the chemical species X, L(X) is the sum of the pseudo-first-order loss rate coefficients of X, and $[X]_{PSSA}$ is the concentration of X in PSS. The system of equations representing each species in the model was solved iteratively using a Gauss-Seidel method (Burden and Faires, 1989). The PCBM of a full $HO_x/NO_x/CH_4$/non-methane-hydrocarbons (NMHCs) system was chemically constrained to 10 minute-averaged values of observed $O_3$, $NO_2$, CO, $SO_2$, and DMS. Detailed description on the PCBM is given in Shon *et al.* (2003). The model contains 59 $HO_x$-$N_xO_Y$-$CH_4$ gas kinetic/photochemical reactions, 146 NMHC reactions, and 12 heterogeneous processes. In the case of nitrogen oxide chemistry, the reactions of $N_2O_5$ and $NO_3$ on aerosol surfaces were considered in the model. The pseudo-first-order loss rate coefficients for the heterogeneous removals of $N_2O_5$ and $NO_3$ radicals ($L_{aero}$) are determined by the uptake coefficient $\gamma$. The loss rate coefficient depends on the chemical composition of the aerosols and temperature (Hu and Abbatt, 1997), total aerosol surface area S per unit volume (in units of $cm^2$ $cm^{-3}$), and the temperature-dependent mean molecular velocity V:

$$L_{aero} = 0.25 \cdot \gamma \cdot V \cdot S \quad (5)$$

The total surface areas during the ADS and NADS periods were estimated to be $1.2 \times 10^{-6}$ and $2.2 \times 10^{-7}$ $cm^2$ $cm^{-3}$, respectively. The values of $4.8 \times 10^{-4}$ and $8.3 \times 10^{-5}$ $s^{-1}$ during ADS and NADS periods were calculated for the $N_2O_5$ loss rate coefficients of the heterogeneous removal ($L_{aero-N_2O_5}$) from equation (5), respectively. $NO_3$ and $N_2O_5$ can also be removed by dry deposition to the ground in the BL. For the calculation of pseudo-first-order loss rate coefficients for the dry deposition of $N_2O_5$ and $NO_3$ radicals, the value of 0.33 cm $s^{-1}$ was taken for the dry deposition velocity from Geyer *et al.* (2001b). In addition, the conversion of $NO_2$ into HONO on aerosol surfaces was considered in the model (Harris *et al.*, 1982). This heterogeneous reaction is implemented with the following loss rate coefficient:

$$L_{NO_2-het} = 5 \times 10^{-3} \text{ cm } s^{-1} \cdot S \quad (6)$$

This rate coefficient is based on a recent tunnel study (Kurtenbach *et al.*, 2002). S value of $1 \times 10^{-3}$ $cm^2$ $cm^{-3}$ was taken from Vogel *et al.* (2003) for the significance test of this heterogeneous process. The value of $2.6 \times 10^{-22}$ $cm^3$ $molecules^{-1}$ $s^{-1}$ was used for the gas-phase reaction rate constant of $N_2O_5$ with $H_2O$ (Wahner *et al.*, 1998; Mentel *et al.*, 1996). The NMHC chemistry scheme adopted here uses the approach of lumping species by chemical family (Lurmann *et al.*, 1986). A detailed description of the PCBM is given in Shon (1999).

Rate constants for the gas-phase reactions and absorption cross-sections for photolysis reactions were taken from Atkinson *et al.* (2001) and the JPL Publications 02-25 (Sander *et al.*, 2002). The actinic flux can be influenced by clouds that increase the backscattered fraction of incident solar radiation, enhancing it above them (de Arellano *et al.*, 1994; van Weele and Duynkerke, 1993; Madronich, 1987). The clouds also increase the actinic fluxes in cloud layers and decrease them below cloud layers (de Arellano *et al.*, 1994; van Weele and Duynkerke, 1993; Madronich, 1987). Scattering aerosols in the BL accelerate photochemical reactions/J values within and above the aerosol layer, while absorbing aerosols decrease J values (Jacobson, 1998; Dickerson *et al.*, 1997). In our model simulation, the corrections for other J values due to aerosols and/or cloud were made based on J ($NO_2$) during the ADS and NADS periods. The effects of dust particles and clouds

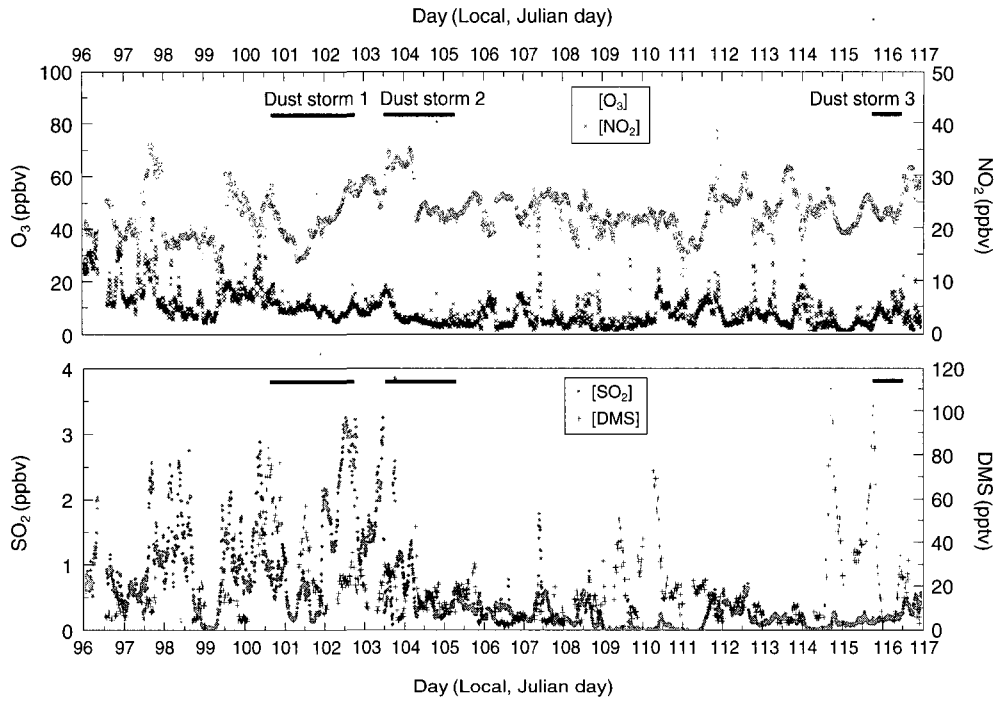


**Fig. 2. Time series of $O_3$, $NO_2$, DMS, and $SO_2$ on Gosan, Jeju Island in the month of April 2001 during the ACE-Asia experiment. Observations for these four species represent 10~15 minute averages. Open circle (○), cross (×), plus (+), and solid circle (●) represent $O_3$, $NO_2$, DMS, and $SO_2$, respectively.**

on J values during the ADS period were taken into account using direct, diffuse, and total solar irradiances obtained at the Gosan station. All photolysis rate coefficients during three ADS periods were adjusted using an averaged correction factor of 0.85 for the cloud and aerosol effect on J values, while those during the NADS period were also adjusted using a correction factor of 0.92. Since NMHCs measurements at the Gosan site were not available, their concentrations were substituted with the previously observed values (C.-H. Kang, private communication, 2002).

## 4. RESULTS AND DISCUSSION

### 4. 1 Comparison of $O_3$, $NO_2$, DMS, and $SO_2$ between the ADS and NADS periods

Time series of $O_3$, $NO_2$, DMS, and $SO_2$ in the ABL in the month of April 2001 are given in Fig. 2. Three ADS events were observed during our study period which include: (1) 1306 LST (local sun time) 10 April (Julian Day (JD) = 100)-1800 LST 12 April (JD = 102), (2) 0912 LST 13 April (JD = 103)-1050 LST 14 April (JD = 105), and (3) 1116 LST 25 April (JD = 115)-0225 LST 26 April (JD = 116). In general, $O_3$ levels during the ADS period were statistically different from those during the NADS period (z-test, P-value = 0 at 95% confidence) (see Table 2 and Fig. 2). For example, $O_3$ concentration during three ADS events was $42 \pm 8$, $59 \pm 9$, and $48 \pm 3$ ppbv, respectively, whereas during the NADS period, it recorded $46 \pm 8$ ppbv. These values were similar to those measured previously at the same site during March through April 1994 (e.g., 55 ppbv, Kim *et al.*, 1998).

Diurnal variation of ozone during the study period is shown in Fig. 3. Between 2250-0720 LST, the $O_3$

**Table 2. The observed concentrations of $O_3$, $NO_2$, DMS, and $SO_2$ during three ADS events and NADS.**

| Species | ADS events | | | NADS periods |
|---|---|---|---|---|
| | ADS 1 | ADS 2 | ADS 3 | |
| $O_3$ (ppbv) | 42(42)±8 | 59(64)±9 | 48(48)±3 | 46(45)±8 |
| $NO_2$ (ppbv) | 4.7(4.5)±1.4 | 4.2(3.0)±2.2 | 2.7(2.6)±1.4 | 4.4(3.4)±3.6 |
| DMS (pptv) | 34(29)±19 | 18(19)±9 | 52(56)±29 | 17(13)±15 |
| $SO_2$ (ppbv) | 1.1(0.8)±0.9 | 1.0(0.8)±0.7 | 0.2(0.1)±0.04 | 0.5(0.3)±0.5 |

The numbers in parenthesis are median values for each chemical species.

levels during the ADS were significantly higher than those during the NADS period, especially 0000-6000 LST (t-test, P-value = $2.3 \times 10^{-22}$). However, there was no significant difference in $O_3$ concentrations during a daytime period between the ADS and NADS. It appears that at near sunrise and sunset, there are sudden decreases in ozone for the ADS with respect to NADS, especially near sunrise. The ozone decreasing phenomenon at near sunrise is likely to be explained by the diurnal variation pattern of $HO_2$ over those time periods, assuming that physico-chemical destruction of ozone and entrainment from the free troposphere are nearly constant during the day. Ozone is chemically removed predominantly by the reactions of $O_3+h\nu \rightarrow O^1D$ , $HO_2+O_3$ , and $OH+O_3$. Only at these periods, the diurnal $HO_2$ profile follows the trend of the sudden drops in ozone at near sunrise and sunset rather than J ($O^1D$) and OH. Even though there was no significant difference in 24-hr averaged $HO_2$ concentrations between the ADS and NADS, $HO_2$ concentrations at near sunrise during the ADS period were higher than those during the NADS period by a factor of 1.8. Ozone decrease in the first few hours following sunrise was revealed based on an analysis of 13 years of observations in the MBL at Cape Grim, Tasmania, implying that ozone destruction at sunrise arises due to halogen chemistry (Galbally *et al.*, 2000). In a recent field study, ozone destruction was also observed just after sunrise in the sub-tropical MBL over the North Pacific, suggesting the cause of halogen chemistry associated with sea-salt aerosols (Nagao *et al.*, 1999). In addition, a model study suggested that the halogen chemistry could significantly affect ozone levels during early

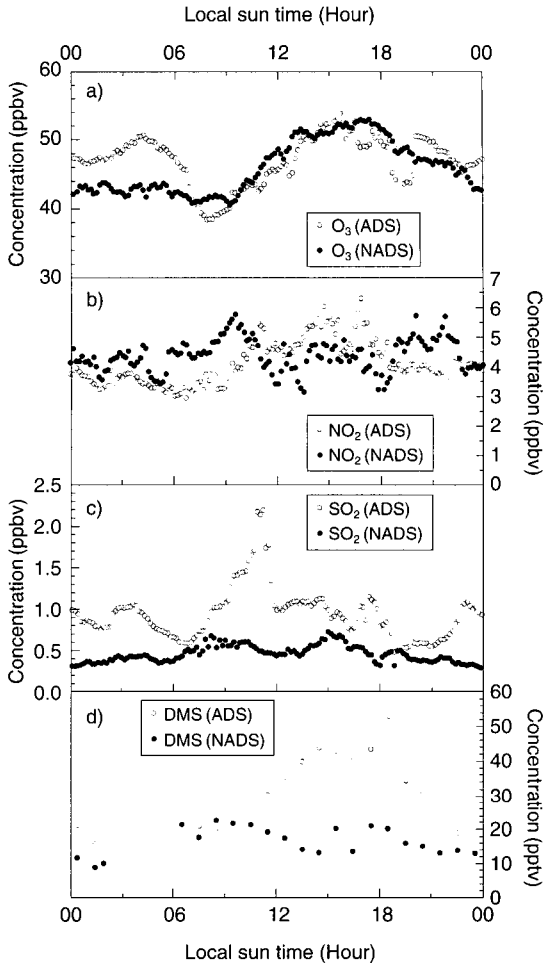


**Fig. 3. Diurnal variations of (a) $O_3$, (b) $NO_2$, (c) DMS, and (d) $SO_2$ during ADS and NADS periods.**

morning after sunrise (Shon and Kim, 2002). Therefore, the possibility of halogen chemistry cannot be excluded as the cause of ozone drop at near sunrise during ADS. Meanwhile, an important aspect of the effect of aerosols on photolysis is ozone photolysis changes.

In the case of $NO_2$, its concentration pattern between the ADS and NADS was similar to that of $O_3$. For example, $NO_2$ concentrations during three ADS events were 4.7±1.4, 4.2±2.2, and 2.7±1.4 ppbv, respectively; during the NADS period, it was 4.4±3.6 ppbv. During the three ADS events, $NO_2$ levels in the third dust-storm event were significantly lower than those

seen in the first and second events (P-value = 0). These $NO_2$ levels on Jeju Island were two orders of magnitude higher than those in the remote MBL. There does appear to be higher $NO_2$ concentrations for the NADS periods in the morning and night (see Fig. 3). The ADS is only higher than NADS in $NO_2$ levels between 1100 and 1800 LST. It appears that ozone decrease at near sunrise shows a corresponding peak in $NO_2$ during the ADS period, indicating anticorrelation between ozone and $NO_2$ (correlation coefficient of −0.75). As anticipated by the fact that NO reacts with ozone to generate $NO_2$ during the daytime, we observed the anticorrelation between ozone and $NO_2$ in our data sets.

In general, DMS levels during the ADS period were statistically higher than those during NADS period by factors of 2.0 to 3.1 (see Table 2). For example, mean DMS values during three ADS events were $34 \pm 19$, $18 \pm 9$, and $52 \pm 29$ pptv, respectively, while that during the NADS period was $17 \pm 15$ pptv. The mean DMS values during the first and third ADS events were statistically higher than those during the NADS period, whereas the mean value during the second event was not. The higher DMS levels during the ADS period resulted from the higher DMS flux over the period than those during the NADS period by a factor of 2. Detailed discussion on DMS photochemistry during the study period is given in Shon *et al.* (in preparation). $SO_2$ concentrations during the NADS period were statistically higher than those during two ADS events by a factor of 2, except for the third event. For example, $SO_2$ concentrations during three ADS events were $1.1 \pm 0.9$, $0.9 \pm 0.7$, and $0.1 \pm 0.04$ ppbv, respectively; during the NADS period it was $0.5 \pm 0.5$ ppbv. Over most of the day, $SO_2$ levels during the ADS period were higher than those during the NADS by a factor of ~2, especially between 0700-1200. During the ADS period, $SO_2$ levels in the third dust-storm event were also significantly less than those seen in the first and second events, implying that $SO_2$ concentrations were sensitive to the air mass trajectories.

The movement patterns of air masses during the sampling period can be put into 4 categories based on air mass back-trajectory analysis: (1) Russia and the East Sea, (2) mainland China and the Yellow Sea, (3) the northeastern China Sea, and (4) the northwestern Pacific (Kim *et al.*, 2003). For example, the air mass passed through eastern China during the first and second ADS, whereas it passed through the less industrialized northern China during the third ADS (Fig. 4). The trajectories of moving air during the NADS period were diverse, compared to those during the ADS period. Table 3 shows the observed concentrations of $O_3$,

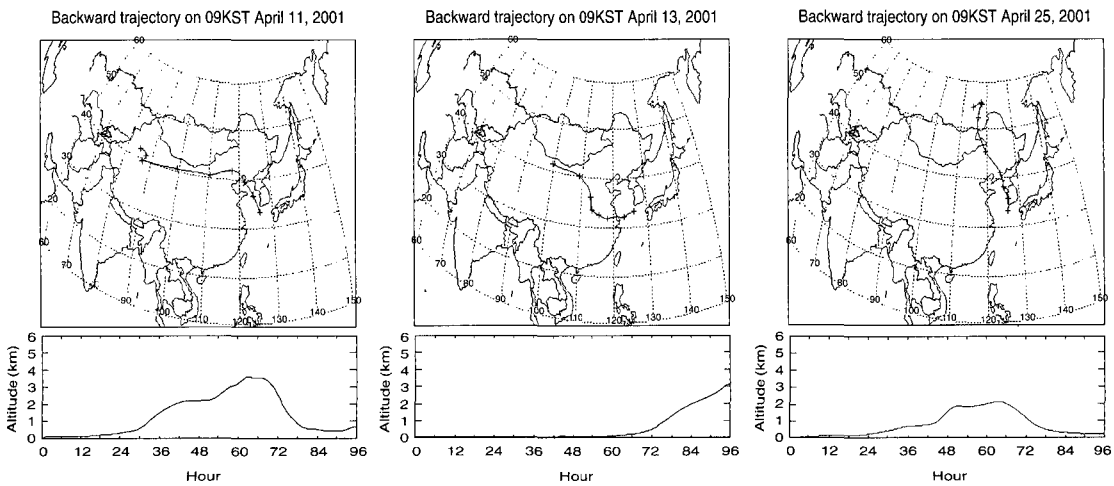


**Fig. 4. Four-day back trajectory analysis for three ADS events at Gosan, Jeju Isand during the study period.**

**Table 3. The observed concentrations of $O_3$, $NO_2$, DMS, and $SO_2$ for each air mass trajectory**

| Species | Air mass (1) | Air mass (2) | Air mass (4) |
|---|---|---|---|
| $O^3$ (ppbv) | 42±14 | 50±10 | 43±7 |
| $NO_2$ (ppbv) | 8.0±5.4 | 3.8±1.8 | 3.0±2.7 |
| DMS (pptv) | 10±5 | 20±10 | 18±15 |
| $SO_2$ (ppbv) | 0.8±0.6 | 1.1±0.9 | 0.2±0.2 |

$NO_2$, DMS, and $SO_2$ for each air mass trajectory. In general, $NO_2$ and $SO_2$ levels in the maritime air mass were significantly lower than those in semi-polluted air mass, whereas DMS concentrations did not show a clear trend depending on air mass origin. $SO_2$ levels on Jeju Island during ACE-Asia were close to previous measurements at the same site during March-April 1994 (Kim *et al.*, 1998).

## 4. 2 Comparison of $NO_3$ estimates between the ADS and NADS periods

Fig. 5 shows the diurnal variation of $NO_3$ radicals calculated using the PCBM for both ADS and NADS periods. In the rural continental and marine BLs, the results of several observations suggested that $NO_3$ is removed by two other mechanisms: (1) its direct homogeneous reactions with organic species (DMS, monoterpenes, isoprene, etc.) and NO and its heterogeneous processes and (2) indirectly via sinks of $N_2O_5$ (homogeneous and heterogeneous reactions), which is generally in a thermodynamical equilibrium with $NO_3$ and $NO_2$ (Geyer *et al.*, 2001b; Allan *et al.*, 2000, 1999; Carslaw *et al.*, 1997; Heintz *et al.*, 1996). For the $NO_3$ inorganic scheme used in the PCBM, we considered a gas phase reaction of DMS+$NO_3$ and three heterogeneous reactions of $NO_3$, $N_2O_5$, and $NO_2$ on aerosol surfaces. Compared to NADS, 5~6 times higher values were used for the pseudo-first-order loss rate coefficients for the heterogeneous reactions during the ADS mainly due to higher total surface area. There were clear differences in $NO_3$ levels between the ADS and NADS periods. The model calculated $NO_3$ levels during the ADS period were lower than those during the NADS period by a factor of 2.8. The average $NO_3$ concentrations at night during ADS and NADS periods were 9 and 27 pptv, respectively. As shown in Fig. 5, the effects of the daytime photolysis of $NO_3$ are clearly apparent at sunset and sunrise. There were no significant differences in $NO_2$ and $O_3$ concentrations between the ADS and NADS (see Table 2), which affect the formation of the $NO_3$ radical. The similar level of $NO_3$ concentrations in semi-polluted air masses (e.g., 8~10 pptv) were also observed in the MBL over the coast of north Norfolk, England (Allan *et al.*, 1999) and at a rural site in the Baltic Sea (Heintz *et al.*, 1996). Even higher $NO_3$ levels (up to 85 pptv) have been reported in the continental BL near Berlin (Geyer *et al.*, 2001a). The causes of significantly lower $NO_3$ concentrations during the ADS appear to be related to a combination of an enhancement of the heterogeneous chemistry for $N_2O_5$, higher DMS concentrations (e.g. by a factor of 1.9), and lower temperature (2.3° K difference). Geyer and Platt (2002) introduced the temperature dependent $NO_3$ loss frequency, $f_{NO_3}$, which arise from the temperature dependence of kinetic constants and of the monoterpene emission rates, as a new indicator for the sink distribution of $NO_3$. The nighttime temperature during ADS was 1.7 K lower than during the NADS. When this temperature difference is applied to $f_{NO_3}$ parameterization derived by Geyer and Plattt (2002), the loss frequency for $NO_3$ from an indirect removal pathway

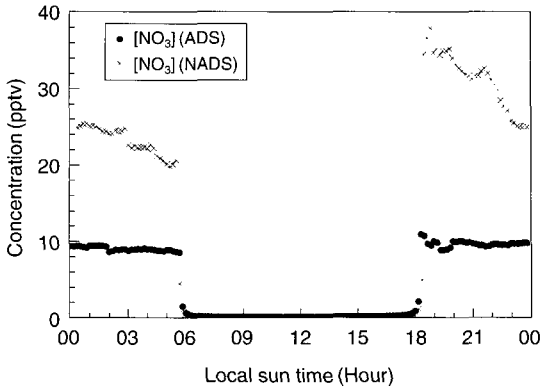


**Fig. 5. Diurnal variation of nitrate radicals during ADS and NADS periods.**

(via $N_2O_5$) during the ADS is about 30% higher than during the NADS and that from the monoterpene reaction during the ADS is about 2% lower. Detailed discussion on the source and sink strengths of $NO_3$ is given in section 4.3.

### 4. 3 Sources and sinks of $NO_3$

The source and sink strengths of $NO_3$ were calculated during the ADS and NADS periods using the PSSA (see Table 4). The dominant source of nitrate radical in the MBL is the reaction of $NO_2$ with ozone. During daytime, nitrate radical concentrations remain low because of rapid photolysis and the fast reaction with NO. However, after sunset they can reach values of several hundred ppt (Geyer *et al.* 2001a; Allan *et al.*, 2000). Nighttime averaged $NO_3$ production rates during the ADS and NADS periods were $3.0 \times 10^6$ and $3.1 \times 10^6$ molecule $cm^{-3}$ $s^{-1}$, respectively. It can be seen that the reaction of $N_2O_5$ on aerosol surfaces was the most important sink for $NO_3$ during the ADS and NADS periods which on nighttime average, constituted 57% and 29% of the total loss, respectively (see Table 4). This is agreeable to a previous study in the MBL for the continental air masses with little marine influence (Allan *et al.*, 2000). In continental BL, $N_2O_5$ on aerosol surface or reactions with NMHCs were the dominant sinks of $NO_3$ (Geyer *et al.*, 2002b, 2001a). By contrast, in the clean MBL, most of $NO_3$ is removed by reaction with DMS (Allan *et al*, 2000; Carslaw *et al.*, 1997). The gas phase reactions of $NO_3$+NMHCs, $NO_3$+DMS, and $N_2O_5$+$H_2O$ during the ADS constitute 10%, 8%, and 7%, on nighttime average, respectively, while those during the NADS constitute 28%, 10%, and 25%, respectively. Dry deposition of $N_2O_5$ and $NO_3$ and the heterogeneous reaction of $NO_3$ were of no importance during both periods. The cause of a predominant $NO_3$ removal mechanism in the ADS appears to be the significant loading of dust particles. $L_{aero}$ for $N_2O_5$ uptake on aerosol surfaces during the ADS is higher than that during the NADS by a factor of 5.5.

**Table 4. The sources and sinks of nighttime $NO_3$ in the MBL (in molecules $cm^{-3}$ $s^{-1}$) using photostationary state calculations**

| Processes | Magnitude | |
|---|---|---|
| Sources | | |
| | ADS | NADS |
| $NO_2+O_3$ | $3.0 \times 10^6$ | $3.1 \times 10^6$ |
| Sinks | | |
| | ADS | NADS |
| $N_2O_5$ uptake on aerosols | $1.7 \times 10^6$ | $9.0 \times 10^5$ |
| $N_2O_5+H_2O$ (gas-phase) | $2.3 \times 10^5$ | $7.8 \times 10^5$ |
| Dry deposition of $N_2O_5$ | $1.3 \times 10^4$ | $3.5 \times 10^4$ |
| $NO_3$+NMHCs | $3.1 \times 10^5$ | $8.6 \times 10^5$ |
| $NO_3$+DMS | $2.4 \times 10^5$ | $3.1 \times 10^5$ |
| Dry deposition of $NO_3$ | $8.0 \times 10^2$ | $2.3 \times 10^3$ |
| $NO_3$ uptake on aerosols | $6.9 \times 10^2$ | $3.8 \times 10^2$ |

### 4. 4 Model Sensitivity

$NO_3$ levels are influenced by several physical and chemical variables that affect both photochemical production and loss rates as well as physico-chemical loss rate. Therefore, the PCBM used for the prediction of $NO_3$ is sensitive to several key input parameters. In order to explore the magnitude of systematic errors in our $NO_3$ estimation, the model sensitivity was checked against each major variable (i.e., [$NO_2$], [NMHC], and $N_2O_5$ uptake coefficient on aerosols). The procedure for the sensitivity tests involved the modification of each variable by a factor of 2 (increase and decrease) to examine the effects on the calculated $NO_3$ concentrations. For [$NO_2$], a positive correlation of 10% variation in nighttime $NO_3$ was calculated. When the NMHC chemistry was not considered, nighttime $NO_3$ increased by a factor of 1.1. For the $N_2O_5$ uptake coefficient on aerosols, an order of magnitude increase of $\gamma_{N_2O_5}$ made significant reduction in $NO_3$ concentrations by a factor of 5 during the ADS. Exclusion of the DMS reaction also made 10% $NO_3$ enhancement. Without consideration of the heterogeneous reactions of $NO_3$, $N_2O_5$, and $NO_2$ on aerosol surfaces, there was $NO_3$ enhancement in the model calculations by a factor of 3 during the ADS. Based on simple calculations, overall uncertainties of $NO_3$ were estimated at 70% and 20%, respec-

tively.

## 5. CONCLUSIONS

The photostationary state method was used to examine the diurnal variation of $NO_3$ under conditions affected by the long-range transport of air pollutants as well as dust particles from the East Asian continent during ADS events. Three ADS events were observed at our study site of Gosan, Jeju Island during the ACE-Asia experiment. Short-term (21 days) observations of $O_3$, $NO_2$, DMS, and $SO_2$ in the MBL indicated that most of these chemical species concentrations were statistically different between the ADS and NADS periods. During the three ADS events, $NO_2$ and $SO_2$ levels in the third dust-storm event were significantly less than those seen in the earlier events, implying that their levels were affected sensitively by the differences in air mass trajectories. The model calculated concentration level of $NO_3$ during the ADS period was significantly lower than those during the NADS period. Decreases in $NO_3$ levels during the ADS period appear to be regulated mainly by enhancement of the $N_2O_5$ heterogeneous reaction. In addition, higher DMS concentrations and lower temperature affected $NO_3$ levels. Nighttime $NO_3$ levels on Jeju Island during the study period were 9~27 pptv. For the $NO_3$ sink, the reaction of $N_2O_5$ on aerosol surfaces was the most important sink for $NO_3$ during the ADS due to higher loading of dust particles. This study suggested that photochemistry of $NO_3$ in the MBL during the ADS was significantly affected by the significant loading of dust aerosols via the heterogeneous chemistry.

## ACKNOWLEDGMENTS

This research was supported by the Dong-Eui University Grant (2002AA010). The authors would like to thank NOAA/ARL and NOAA/CMDL for providing HYSPLIT model, meteorological data, and solar radiation radiometer data. The authors would like to thank Dr. Swan at AGAL, Australia for providing DMS data. The authors would like to thank Dr. Chuang at UCSC for providing NOAA Climet OPC processed data. The authors would like to thank Dr. C.-H. Kang for providing NMHCs historical data.

## REFERENCES

Allan, B.J., N. Carslaw, H. Coe, R.A. Burgess, and J.M.C. Plane (1999) Observations of the nitrate radicals in the marine boundary layer, J. Atmos. Chem., 33, 129-154.

Allan, B.J., McFiggans, J.M.C. Plane, H. Coe and G.G. McFadyen (2000) The nitrate radical in the remote marine boundary layer, J. Geophys. Res., 105, 24191-24204.

Atkinson, R., D.L. Baulch, R.A. Cox, J.N. Crowley, Jr. R.F. Hampson, J.A. Kerr, M.J. Rossi, and J. Troe (2001) Summary of Evaluated Kinetic and Photochemical Data for Atmospheric Chemistry, Web Version December 2001, www.iupac-kinetic.ch.cam.ac.uk, University of Cambridge, UK.

Burden, R.L., and J.D. Faires (1989) Numerical Analysis, PWS Kent, Boston.

Carslaw, N., L.J. Carpenter, J.M.C. Plane, B.J. Allan, R.A. Burgess, K.C. Clemitshaw, and S.A. Penkett (1997) Simultaneous observations of nitrate and peroxy radicals in the marine boundary layer, J. Geophys. Res., 102, 18917-18933.

Carslaw, N., D.J. Creasey, D.E. Heard, A.C. Lewis, J.B. McQuaid, M.J. Pilling, P.S. Monks, B.J. Bandy, and S.A. Penkett (1999) Modeling OH, $HO_2$, and $RO_2$ radicals in the marine boundary layer, 1. Model construction and comparison with field measurements, J. Geophys. Res., 107, D14, 10.1029/2001JD001568.

De Arellano, J.V.-G., P.G. Duynkerke, and M. Van Weele (1994) Tethered-balloon measurements of actinic flux in a cloud-capped marine boundary layer, J. Geophys. Res., 99, 3699-3705.

Dickerson, R.R., S. Kondragunda, G. Stenchikov, K.L. Civerolo, B.G. Doddrigde, and B.N. Holben (1997) The impact of aerosols on solar UV radiation and photochemical smog, Science, 278, 827-830.

Galbally, I.E., S.T. Bentley, and C.P. Meyer (2000) Mid-latitude marine boundary-layer ozone destruction at visible sunrise observed at Cape Grim, Tasmania, 41° S, Geophys. Res. Lett., 27, 3841-3844.

Geyer, A., R. Ackermann, R. Dubois, B. Lohrmann, T. Müller, and U. Platt (2001a) Long-term observation of nitrate radicals in the continental boundary layer near Berlin, Atmos. Environ., 35, 3619-3631.

Geyer, A., B. Alicke, S. Konrad, T. Schmitz, J. Stutz, and U. Platt (2001b) Chemistry and oxidation capacity of the nitrate radical in the continental boundary layer near Berlin, J. Geophys. Res., 106, 8013-8025.

Geyer, A. and U. Platt (2002) Temperature dependence of the $NO_3$ loss frequency: A new indicator for the contribution of $NO_3$ to the oxidation of monoterpenes and $NO_x$ removal in the atmosphere, J. Geophys. Res., 107, 4431-4442.

Harris, G.W., W.P.L. Carter, A.M. Winer, J.N. Pits, U. Plat, and D. Perner (1982) Observations of nitrous acid in the Los Angeles atmosphere and implications of the predictions of ozone-precursor relationships, Environ. Sci. Tech., 16, 414-419

Heintz, F., U. Platt, H. Flentje, and R. Dubois (1996) Long-term observations of nitrate radicals at the Tor Station, Kap Arkona (Rügen), J. Geophys. Res., 101, 22891-22910.

Hu, J.H. and J.P.D. Abbatt (1977) Reaction probabilities for $N_2O_5$ hydorlysis on sulfuric acid and ammonium sulfate aerosols at room temperature, J. Phys. Chem., 101, 871-878.

Jacobson, M.Z. (1998) Studying the effects of aerosols on vertical photolysis rate coefficient and temperature profiles over an urban airshed, J. Geophys. Res., 103, 10593-10604.

Jaffee, D., T. Anderson, D. Covert, R. Kotchenruther, B. Trost, J. Danielson, W. Simpson, T. Berntsen, S. Karlsdottir, D. Blake, J. Harris, G. Carmichael, and I. Uno (1999) Transport of Asian Air Pollution to North America, Geophys. Res. Lett., 26, 711-714.

Kim, K.-H., G. Lee, and Y.P. Kim (2000) Dimethylsulfide and its oxidation products in coastal atmospheres of Cheju Island, Environ. Poll., 110, 147-155.

Kim, K.-H., H. Swan, Z.-H. Shon, G. Lee, J. Kim, and C.-H. Kang (in press) Monitoring of natural sulfur compounds in the atmosphere of Kosan, Cheju during the Spring of 2001, Chemosphere.

Kim, Y.P., S.G. Shim, K.C. Moon, C.G. Hu, and C.-H. Kang (1998) Monitoring of air pollutants at Kosan, Cheju Island, Korea, during March ~ April, 1994, J. App. Meteo., 37, 1117-1126.

Kurtenbach, R., R. Ackermann, K.H. Becker, J.C. Lözer, U. Platt, and P. Wiesen (2002) Verification of the contribution of vehicular traffic to the total NMVOC emissions in Germany and the importance of the $NO_3$ chemistry in the city air, J. Atmos. Chem., 42, 395-411.

Lurmann, F.W., A.C. Lloyd, and R. Atkinson (1986) A chemical mechanism for use in long-range transport/acid deposition computer modeling, J. Geophys. Res., 91, 10905-10936.

Madronich, S. (1987) Intercomparion of $NO_2$ photodissociation and U.V. radiometer measurement, Atmos. Environ., 21, 569-578.

Mentel, T.F., D. Bleilebens, and A. Wahner (1996) A study of nighttime nitrogen oxide oxidation in a large reaction chamber-the fate of $NO_2$, $N_2O_5$, $HNO_3$, and $O_3$ at different humidities, Atmos. Environ., 30, 4007-4020.

Nagao, I., K. Matsumoto, and H. Tanaka (1999) Sunrise ozone destruction found in the sub-tropical marine boundary layer, Geophys. Res. Lett., 26, 3377-3380.

Sander, S.P., R.R. Friedl, D.M. Golden, M.J. Kurylo, R.E. Huie, V.L. Orkin, G.K. Moortgat, A.R. Ravishankara, C.E. Kolb, M.J. Molina, and B.J. Finlayson-Pitts (2002) Chemical kinetics and photochemical data for use in stratospheric modeling, JPL Publication 02-25, Jet Propulsion Laboratory, California Institute of Technology, Pasadena, California.

Shon, Z.-H. (1999) Photochemical assessment of oceanic emissions of DMS and its oxidation to $SO_2$ based on airborne field observations. Ph. D. dissertation, Georgia Institute of Technology, Atlanta, GA, USA.

Shon, Z-H., K.-H. Kim, K.N. Bower, G. Lee, and J. Kim (in press) Assessment of the Photochemistry of OH and $NO_3$ on Jeju Island during the Asian Dust-Storm Period in the Spring of 2001, Chemosphere.

Shon, Z.-H., K.-H. Kim, H. Swan, G. Lee, and Y.K. Kim (submitted) Assessment of DMS photochemistry on Jeju Island During the Asian Dust-Storm Period of Spring 2001: Comparison of Model Simulations with Field Observations.

Shon, Z.-H. and N. Kim (2002) A modeling study of halogen chemistry's role in marine boundary layer ozone,

Atmos. Environ., 36, 4289-4298.

Swan, H.B. and J.P. Ivey (1999) Evaluation of two sulfur specific detectors for the measurement of dimethylsulfide gas concentrations at Macquarie island and Cape Grim during ACE-1, In Baseline Atmospheric Program (Australia) 1996, 15-23.

van Weele, M. and P.G. Duynkerke (1993) Effect of clouds on the photodissociation of $NO_2$: Observations and modeling, J. Atmos. Chem., 16, 231-255.

Vogel, B., H. Vogel, J. Kleffmann, and R. Kurtenbach (2003) Measured and simulated vertical profiles of nitrous acid-Part II. Model simulations and indications for a photolytic source, Atmos. Environ., 37, 2957-2966.

Wahner, A., T.F. Mentel, M. Sohn, and J. Stier (1998) Heterogeneous reaction of $N_2O_5$ on sodium nitrate aerosol, J. Geophys. Res., 103, 31103-31112.

Wayne, R.P. (1991) Chemistry of Atmosphere, Oxford Science, New York.

Wayne, R.P., I. Barnes, P. Biggs, J.P. Burrows, C.E. Canosa-Mas, J. Hjorth, G. Le Bras, G.K. Moortgat, D. Perner, G. Poulet, G. Restelli, and H. Sidebottom (1991) The nitrate radical: Physics, chemistry, and the atmosphere, Atmos. Environ., 25, 1-203.